Progress In Electromagnetics Research B, Vol. 3, 143–156, 2008

ANALYSIS OF PERIODICALLY LOADED SUSPENDED SUBSTRATE STRUCTURES IN MILLIMETER WAVE

M. Fardis and R. Khosravi

Iran Telecommunication Research Center
Communication Technology Institute
P.O. Box 14155-3961, Tehran, Iran

Abstract—This paper presents a comprehensive study on the hybrid mode analysis of a periodic structure in a Suspended Microstrip and Broadside-coupled Suspended Stripline. The analysis has been use of Floquet's theorem in special harmonics to express the field equations in various sub regions of the periodic loaded suspended substrate. Their characteristic equation is derived, using the Galerkin's procedure. The unknown electric field distribution in the substrate region, corresponding to one unit cell of the periodic structure is specified in terms of suitable basis functions. The characteristic of slow wave properties, resonance behavior and the passband-stopband characteristics are at the millimeter wave frequencies as a various structural parameters are presented.

1. INTRODUCTION

Suspended Stripline and Fin Lines are the most popularly used transmission media to realize integrated circuits in millimeter wave bands, frequencies range from 30 GHz up to about 120 GHz. These structures have been studied and reported as uniform transmission lines [1–8]. Periodic transmission lines are basically slow wave structures. They are applicable in high quality filters, high directivity couplers, delay lines, and phase shifters. Their slow wave property permits considerable reduction in component size which can be exploded to realize compact millimeter wave circuit using monolithic technology.

A hybrid mode analysis of a periodically loaded suspended substrate is presented in present paper. Floquet's theorem is applied to express the field equations in various sub regions of periodic suspended substrate. The characteristic equation is then derived, using the

Galerkin's procedure. The unknown electric field distribution in one unit cell of the periodic structure is specified in terms of suitable basis functions. Detailed characteristics of slow wave propagation, resonance and the passband–stopband behaviors are reported at ka-band frequencies as a various parameters of the periodic loaded suspended substrate pattern.

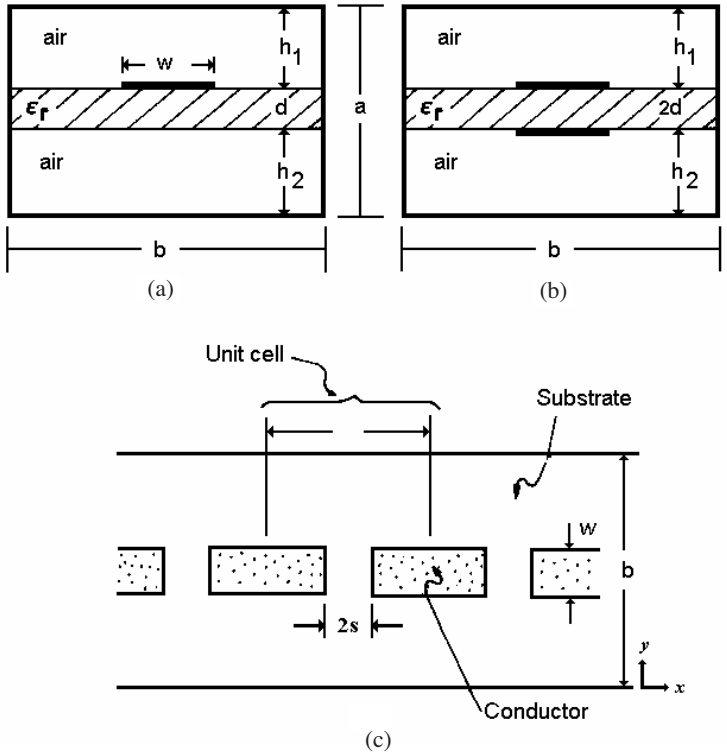

Figure 1. Cross-sectional views of suspended substrate line for periodic structures. (a) suspended stripline ($h_1 \neq h_2$), (b) broadside-coupled suspended stripline, (c) periodic loaded pattern on the substrates.

2. ANALYSIS

Consider the periodically loaded with suspended substrate as is shown in Fig. 1. To make the analysis more simple, one symmetric half of those coupled structures can be considered by placing an electric wall, EW, and a magnetic wall, MW, for the odd and even mode excitation, respectively, at the plane of the symmetry.

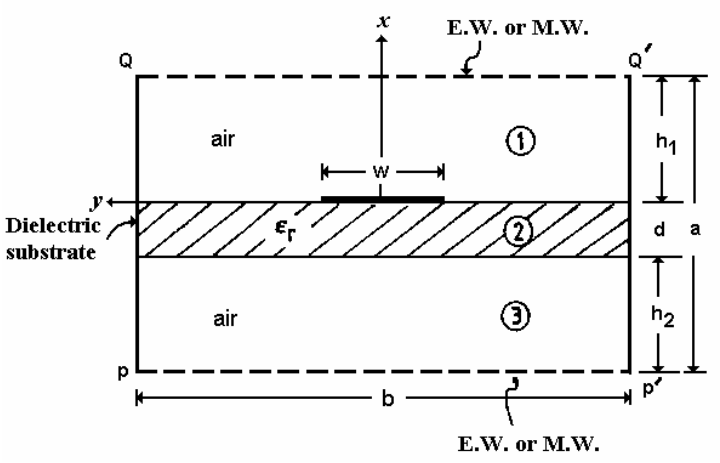

Figure 2. One half of the general suspended stripline with top and bottom walls as Electric or Magnetic walls for analysis.

The x-components of electric and magnetic fields can be driven by the solution of Helmholtz equation in the three homogenous regions (see Fig. 2).

$$E_x^{(1)}=\sum_{m=-\infty}^{\infty}\sum_{n=1}^{\infty}A_{mn1}\cos[\gamma_{mn1}(x-h_1)]\cos(\alpha_n y)e^{-j\beta_m z} \tag{1.1}$$

$$H_x^{(1)}=\sum_{m=-\infty}^{\infty}\sum_{n=0}^{\infty}B_{mn1}\sin[\gamma_{mn1}(x-h_1)]\sin(\alpha_n y)e^{-j\beta_m z} \tag{1.2}$$

$$E_x^{(2)}=\sum_{m=-\infty}^{\infty}\sum_{n=1}^{\infty}[A_{mn2}\sin(\gamma_{mn2}x)+A'_{mn2}\cos(\gamma_{mn2}x)]\cos(\alpha_n y)e^{-j\beta_m z} \tag{1.3}$$

$$H_x^{(2)}=\sum_{m=-\infty}^{\infty}\sum_{n=0}^{\infty}[B_{mn2}\cos(\gamma_{mn2}x)+B'_{mn2}\sin(\gamma_{mn2}x)]\sin(\alpha_n y)e^{-j\beta_m z} \tag{1.4}$$

$$E_x^{(3)}=\sum_{m=-\infty}^{\infty}\sum_{n=1}^{\infty}A_{mn3}\cos[(\gamma_{mn1}(x+d+h_2)]\sin(\alpha_n y)e^{-j\beta_m z} \tag{1.5}$$

$$H_x^{(3)}=\sum_{m=-\infty}^{\infty}\sum_{n=0}^{\infty}B_{mn3}\cos[(\gamma_{mn1}(x+d+h_2)]\cos(\alpha_n y)e^{-j\beta_m z} \tag{1.6}$$

where the super scripts 1, 2 and 3 refer to three regions, marks in

Fig. 2. The other parameters are:

$$\gamma_{mn1} = \sqrt{k_0^2 - (\alpha_n^2 + \beta_m^2)}, \quad \gamma_{mn2} = \sqrt{k_0^2 \varepsilon_r - (\alpha_n^2 + \beta_m^2)} \tag{2.1}$$

$$\alpha_n = (2n+1)\frac{\pi}{b}, \qquad \beta_m = \beta_0 + 2m\frac{\pi}{b} \tag{2.2}$$

β_0 in the dominant mode propagation constant and P is the periodicity, the y-components and z-components of the electric and the magnetic fields can be driven by using (1) in the Maxwell's equations.

$$E_y^{(1)} = \sum_{m=-\infty}^{\infty} \sum_{n=0}^{\infty} s_{mn1} \sin[\gamma_{mn1}(x - h_1)] \sin(\alpha_n y) e^{-jB_m z} \tag{3.1}$$

$$E_y^{(2)} = \sum_{m=-\infty}^{\infty} \sum_{n=0}^{\infty} [s_{mn2} \cos(\gamma_{mn2} x) + S'_{mn2} \sin(\gamma_{mn2} x)] \sin(\alpha_n y) e^{-j\beta_m z} \tag{3.2}$$

$$E_y^{(3)} = \sum_{m=-\infty}^{\infty} \sum_{n=0}^{\infty} s_{mn3} \sin[\gamma_{mn1}(x + d + h_2)] \sin(\alpha_n y) e^{-j\beta_m z} \tag{3.3}$$

$$E_z^{(1)} = \sum_{m=-\infty}^{\infty} \sum_{n=1}^{\infty} C_{mn1} \sin[\gamma_{mn1}(x - h_1)] \cos(\alpha_n y) e^{-j\beta_m z} \tag{3.4}$$

$$E_z^{(2)} = \sum_{m=-\infty}^{\infty} \sum_{n=1}^{\infty} [C_{mn2} \cos(\gamma_{mn2} x) + C'_{mn2} \sin(\gamma_{mn2} x)] \cos(\alpha_n y) e^{-j\beta_m z} \tag{3.5}$$

$$E_z^{(3)} = \sum_{m=-\infty}^{\infty} \sum_{n=1}^{\infty} C_{mn3} \sin[\gamma_{mn1}(x + d + h_2)] \cos(\alpha_n y) e^{-j\beta_m z} \tag{3.6}$$

$$H_y^{(1)} = \sum_{m=-\infty}^{\infty} \sum_{n=1}^{\infty} C_{mn1} \cos[\gamma_{mn1}(x - h_1)] \cos(\alpha_n y) e^{-j\beta_m z} \tag{3.7}$$

$$H_y^{(2)} = \sum_{m=-\infty}^{\infty} \sum_{n=1}^{\infty} [M_{mn2} \cos(\gamma_{mn2} x) + M'_{mn2} \sin(\gamma_{mn2} x)] \cos(\alpha_n y) e^{-j\beta_m z} \tag{3.8}$$

$$H_y^{(3)} = \sum_{m=-\infty}^{\infty} \sum_{n=1}^{\infty} C_{mn3} \sin[\gamma_{mn1}(x + d + h_1)] \cos(\alpha_n y) e^{-j\beta_m z} \tag{3.9}$$

$$H_z^{(1)} = \sum_{m=-\infty}^{\infty} \sum_{n=0}^{\infty} D_{mn1} \cos[\gamma_{mn1}(x - h_2)] \sin(\alpha_n y) e^{-j\beta_m z} \tag{3.10}$$

$$H_z^{(2)} = \sum_{m=-\infty}^{\infty} \sum_{n=0}^{\infty} [D_{mn2} \sin(\gamma_{mn2} x) + D'_{mn2} \cos(\gamma_{mn2} x)] \sin(\alpha_n y) e^{-j\beta_m z} \tag{3.11}$$

$$H_z^{(3)} = \sum_{m=-\infty}^{\infty} \sum_{n=0}^{\infty} C_{mn3} \cos[\gamma_{mn1}(x+d+h_2)] \sin(\alpha_n y) e^{-j\beta_m z} \quad (3.12)$$

In the above field expressions, there are eight unknown coefficients. Applying boundary conditions at $x = 0$ and $x = -d$, the unknown coefficients can be reduced to only A_{mn1} and B_{mn1}.

3. DERIVATION OF CHARACTERISTIC EQUATION

By deriving the characteristic equation of the periodic structure, we need to express the unknown coefficients in terms of the transformed fields. We consider one unit cell of the periodic structure as shown in Fig. 1. Applying the orthogonal condition to unit cell, we obtain,

$$pb\left[\alpha_n C_{mn} B_{mn1} + \beta_m S_{mn} A_{mn1}\right] = L_{2mn}\left[p_n(\alpha_n^2 + \beta_m^2)\right] \quad (4.1)$$

$$pb\left[j\beta_m C_{mn} B_{mn1} - j\alpha_n S_{mn} A_{mn1}\right] = L_{1mn}\left[Q_n(\alpha_n^2 + \beta_m^2)\right] \quad (4.2)$$

where,

$$L_{2mn} = \int_{-p/2}^{p/2} \int_{-b/2}^{b/2} J_z \cos(\alpha_n y) e^{j\beta_m z} dy dz \quad (4.3)$$

$$L_{1mn} = \int_{-p/2}^{p/2} \int_{-b/2}^{b/2} J_y \sin(\alpha_n y) e^{j\beta_m z} dy dz \quad (4.4)$$

$$p_n = \begin{cases} 1 & \text{for } \alpha_n = 0 \\ 2 & \text{otherwise} \end{cases}, \qquad Q_n = \begin{cases} 0 & \text{for } \alpha_n = 0 \\ 2 & \text{otherwise} \end{cases} \quad (4.5)$$

Now by expressing the unknown coefficients A_{mn1} and B_{mn1}, in terms of L_{2mn} and L_{1mn} we obtain,

$$A_{mn1} = \left(\frac{1}{pb}\right)\left[\left(\beta_m P_n L_{2mn} - j\alpha_n Q_n L_{1mn}\right) / \left(S_{mn}\right)\right] \quad (5.1)$$

$$B_{mn1} = \left(\frac{1}{pb}\right)\left[\left(\alpha_n P_n L_{2mn} + j\beta_m Q_n L_{1mn}\right) / \left(C_{mn}\right)\right] \quad (5.2)$$

By considering $E_y^{(1)}$ and $E_z^{(1)}$ at $x = 0$ and substitute the value of A_{mn1} and B_{mn1}, and applying the Galerkin's method in transformed domain, and then eliminate the electric field, the following set of homogenous

equations can be obtained.

$$\sum_{i=-\infty}^{\infty}\sum_{j=1}^{\infty} c_{ij} \sum_{m=-\infty}^{\infty}\sum_{n=1}^{\infty} Q_n G_{11} L_{1mn}^{(i,j)} L_{1mn}^{(k,l)} + \sum_{i=-\infty}^{\infty}\sum_{j=1}^{\infty} d_{ij} \sum_{m=-\infty}^{\infty}\sum_{n=1}^{\infty} P_n G_{12} L_{2mn}^{(i,j)} L_{1mn}^{(k,l)} = 0 \tag{6.1}$$

$$\sum_{i=-\infty}^{\infty}\sum_{j=1}^{\infty} c_{ij} \sum_{m=-\infty}^{\infty}\sum_{n=1}^{\infty} Q_n G_{21} L_{1mn}^{(i,j)} L_{2mn}^{(k,l)} + \sum_{i=-\infty}^{\infty}\sum_{j=1}^{\infty} d_{ij} \sum_{m=-\infty}^{\infty}\sum_{n=1}^{\infty} P_n G_{22} L_{2mn}^{(i,j)} L_{2mn}^{(k,l)} = 0 \tag{6.2}$$

where,

$$k = -\infty \text{ to } +\infty; \qquad l = 1, 2, 3, \ldots, +\infty \tag{6.3}$$

$$L_{2mn}^{(k,l)} = \int_{-p/2}^{p/2}\int_{0}^{b} e_y^{(k,l)}(y,z)\cos(\alpha_n y) e^{-j\beta_m z} dy dz \tag{7.1}$$

$$L_{1mn}^{(k,l)} = \int_{-p/2}^{p/2}\int_{0}^{b} e_z^{(k,l)}(y,z)\sin(\alpha_n y) e^{-j\beta_m z} dy dz \tag{7.2}$$

$$G_{11} = -\sin(\gamma_{mn1} h_1)\left(\frac{j\beta_m^2\gamma_{mn1}}{S_{mn}} - \frac{jw\mu_0\alpha_m^2}{C_{mn}}\right)/\left(\alpha_n^2+\beta_m^2\right) \tag{8.1}$$

$$G_{12} = -\sin(\gamma_{mn1} h_1)\left(\frac{\alpha_n\beta_m\gamma_{mn1}}{S_{mn}} - \frac{w\mu_0\alpha_n\beta_m}{C_{mn}}\right)/\left(\alpha_n^2+\beta_m^2\right) \tag{8.2}$$

$$G_{21} = -G_{12} \tag{8.3}$$

$$G_{22} = -\sin(\gamma_{mn1} h_1)\left(\frac{j\alpha_n^2\gamma_{mn1}}{S_{mn}} - \frac{j\beta_m^2 w\mu_0}{C_{mn}}\right)/\left(\alpha_n^2+\beta_m^2\right) \tag{8.4}$$

To analysis the periodically loaded suspended substrate line, with bottom wall replaced by magnetic wall in Fig. 2 and considering any periodic strips conductor pattern, we note that the solution of Helmholtz equation in regions 1 and 2 is identical to that of the suspended structure. But for region 3, the x-dependent terms represented by "sin", is replaced by "cos" and vice-versa. The same procedures for field equations in the three regions has been followed, and finally by applying Galerkin's method in transformed domain, we obtained the same characteristic equation in the form of a set of homogenous equations (6).

4. FIELD DISTRIBUTION

Referring to the strip conductor pattern, shown in Fig. 2, the basis function strip current distribution in one unit cell of the periodic structure are,

$$e_z(y,z) = 0 \tag{9.1}$$

$$e_y(y,z) = C_{01}e_y^a(y,z) + C_{-11}e_y^b(y,z) \tag{9.2}$$

$$e_y^a(y,z) = e_y^a(y)e_y^a(z) = \left[1 + \left|\frac{1}{w}\left\{y - 2s_1\left(\frac{b-y}{b-w}\right)\right\}\right|^3\right] U(z)e^{-j\beta_0 z}, \quad s_1 < y < s_1 + w \tag{9.3}$$

$$e_y^b(y,z) = e_y^b(y)e_y^b(z) = \left[1 + \left|\frac{1}{w}\left\{y - 2s_1\left(\frac{b-y}{b-w}\right)\right\}\right|^3\right] U(z)e^{-j\beta_{-1} z}, \quad s_1 < y < s_1 + w \tag{9.4}$$

where:

$$e_y^a(y) = e_y^b(y) = \left[1 + \left|\frac{1}{w}\left\{y - 2s_1\left(\frac{b-y}{b-w}\right)\right\}\right|^3\right] = e_y(y) \tag{9.5}$$

$$e_y^a(z) = U(z)e^{-jB_0 z} \tag{9.6}$$

$$ey^b(z) = U(z)e^{-j\beta_{-1} z} \tag{9.7}$$

$$U(z) = \begin{cases} 1 & s < |z| < p/2 \\ 0 & |z| < s \end{cases} \tag{9.8}$$

$$\beta_{-1} = \left(\beta_0 - \frac{2\pi}{p}\right) \tag{9.9}$$

where $e_y^a(y,z)$ and $e_y^b(y,z)$ are the basis functions corresponding to the dominant mode and the first special harmonic, respectively, and C_{01}, C_{-11} are unknown coefficients.

5. NUMERICAL RESULTS

The propagation constants of the structure for the dominate and higher order harmonics are determined by substituting the transformed basis functions for the strip conductor field in the characteristic equation (6) and setting the determinant of the coefficient matrix equal to zero.

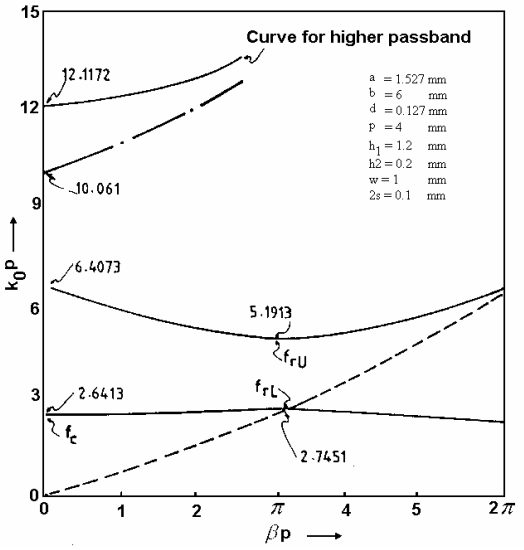

Figure 3. $k_0 - \beta_0$ diagram of suspended stripline periodically loaded with series capacitive gaps.

Figure 3 illustrates a typical $k_0 - \beta_0$ diagram. The first passband occurs in the frequency range when k_0P satisfy $2.4413 < k_0P < 2.7451$ and first stopband occurs in the range of $2.7451 < k_0P < 5.1913$ which demonstrating very narrow passband and wide stopband the curve for the periodically loaded suspended stripline is above that for the uniform suspended stripline because of the capacitive reactance of the series gaps and the higher passband curves $(k_0 - \beta_0)$ of the periodic structure is above that of the uniform line for the higher order mode. Thus, the higher passbands and stopbands are not of much significance. Fig. 4 shows the variation in the stopbandwidth as a function of gap width $2s$ for two different value of stripwidth ($w = 1\,\text{mm}$ and $w = 2\,\text{mm}$). The periodicity is held fixed at $P = 4\,\text{mm}$. Thus as $2s$ is increased, the strip conductor length l decreases. Consequently, the resonant frequency f_{rL} increases. Fig. 4 also shows that an increase in $2s$ from 0.5 mm to 2 mm, f_{rL} increases where as the stopband width remains wide and fairly constant.

Figure 5 shows the variation in the effective dielectric constant as a function of frequency for different combinations of w, $2s$ and P. It also illustrates similar graph for different combinations of h_1 and h_2.

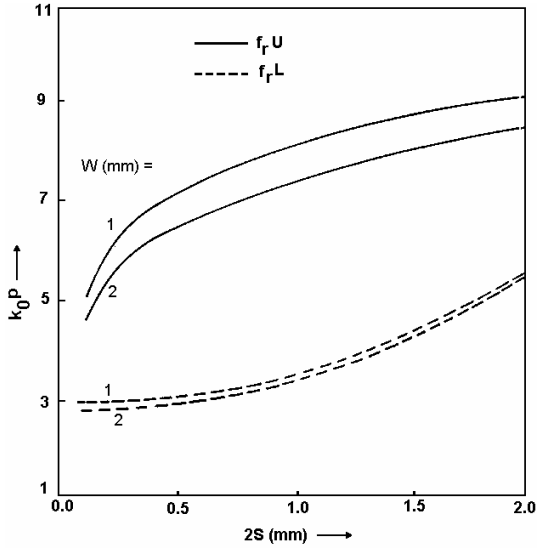

Figure 4. Effect of capacitive gap loading on the upper and lower frequency bounds (f_{rU} and f_{rL}) of the first stopband in suspended stripline periodically loaded with series capacitive gaps.

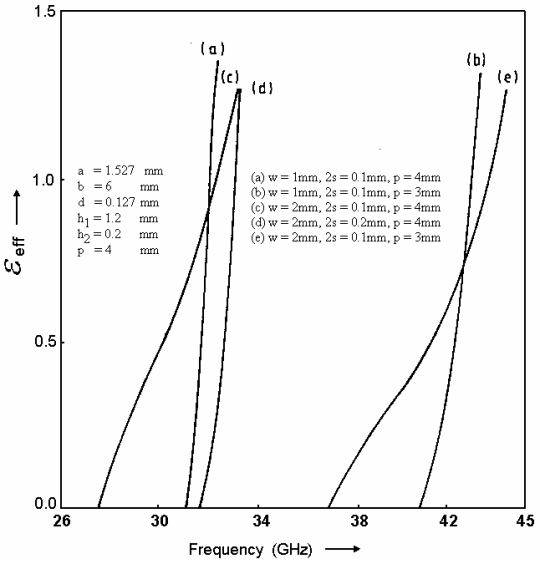

Figure 5. Dispersion of suspended stripline periodically loaded with series capacitive gaps for different combination of w, $2s$ and P.

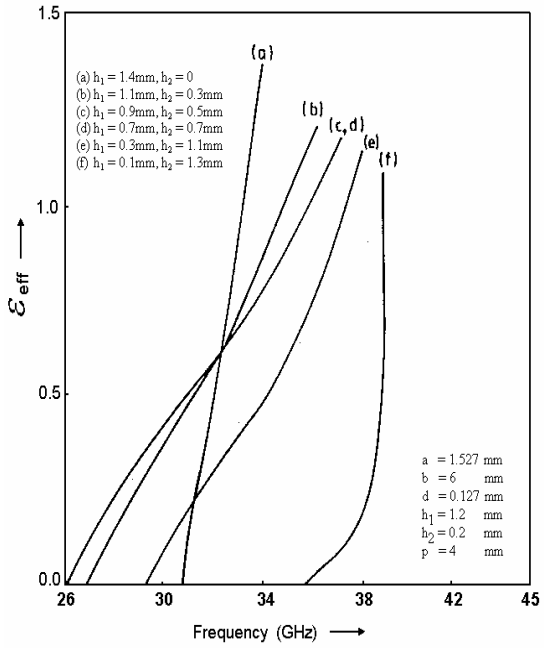

Figure 6. Dispersion of suspended stripline periodically loaded with series capacitive gaps for different combination of h_1 and h_2.

Each curves in these figures corresponds to passband filter response. The frequencies corresponding to $\varepsilon_{eff} = 0$ give the cutoff frequencies and can be read from the horizontal axis. Also from Fig. 6, the curves marked a, b and d which are for $2s/w = 0.1$ shows extremely narrow passband and curves c and e which are for lower value of $2s/w = 0.05$ show wider passband, curve c is for $P = 4\,\text{mm}$ and curve e is for $P = 3\,\text{mm}$. As expected, reducing the periodicity has the effect of shifting the passband to higher frequency.

In Fig. 5, with $2s/w = 0.05$ and $P = 4\,\text{mm}$ we consider the effect of varying the air gap h_1 (in which $h_2 = a - (d + h_1)$, a and d are fixed) on the dispersion characteristics, when in curve a, $h_2 = 0$ (microstrip) and curve f when the strip conductor in extremely close to the topwall ($h_1 = 0.1\,\text{mm}$) very narrow passband results, where the strip conductor pattern is in close proximity to the bottom or top wall. Furthermore, the passband response shifts towards higher frequency, and curves b, c, d and e which show larger passband, refer to cases for which the strip conductor pattern in sufficiently away from the top and bottom walls. Curve d refers to the symmetric suspended stripline ($h_1 = h_2 = 0.7\,\text{mm}$). Lowering the substrate from the centre

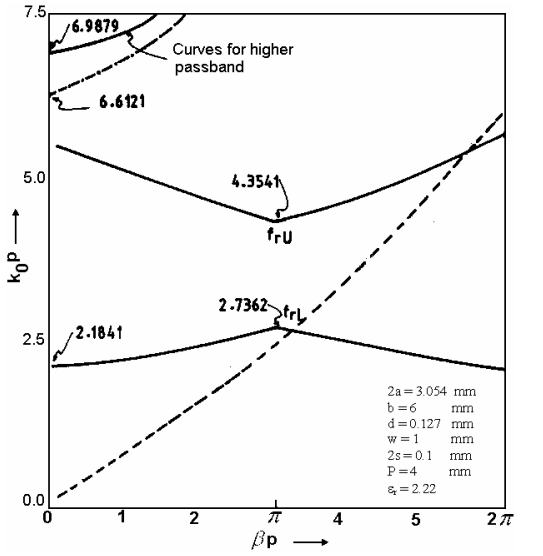

Figure 7. $k_0 - \beta_0$ diagram of broadside-coupled suspended stripline periodically loaded with series capacitive gaps.

by 0.2 mm (i.e., $h_2 = 0.5$ mm) has practically no effect on dispersion characteristic.

The nature of $k_0 - \beta_0$ diagram in broadside-coupled suspended stripline periodically loaded with series capacitive gaps with even mode excitation which is showing in Fig. 7, is similar to that of Fig. 3. The fact that the first passband starts from a finite value of k_0P not zero, is characteristic of the periodic pattern.

The effect of series gap loaded as shown in Fig. 8, we observe that the stopband width which is initially zero for $2s = 0$ (uniform line) increases first with an increase in $2s$ and then decrease with fixing periodicity an increase in $2s$, both f_{rU} and f_{rL} increase, and beyond a certain value of $2s$, which f_{rL} continuous to increase, f_{rU} saturates thereby reducing the stopband width. For a sufficiently large value of $2s$ when the adjacent strip conductors get increasing by decoupled f_{rL} approaches the value of f_{rU}.

Figure 9 illustrates the dominant mode passband resonance. Curves c and d which are for wider strips ($w = 2$ mm) show the similar slope. The curves a and b which are for narrower strips ($w = 1$ mm). These curves in conjunction with the $k_0 - \beta_0$ diagram (Fig. 7) shows

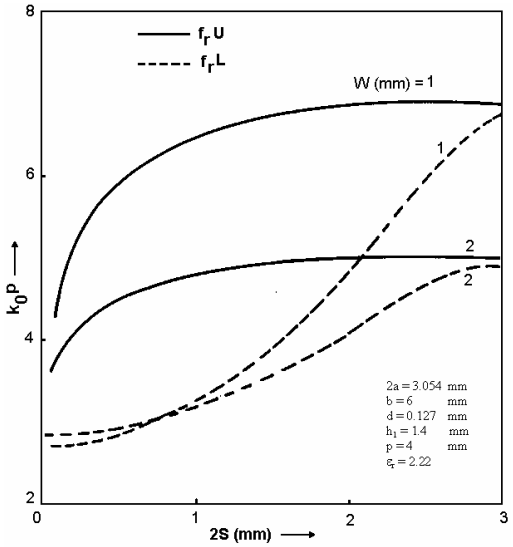

Figure 8. Effect of series gap loading on the upper and lower frequency bounds of the first stopband in broadside-coupled suspended stripline periodically loaded with series capacitive gaps.

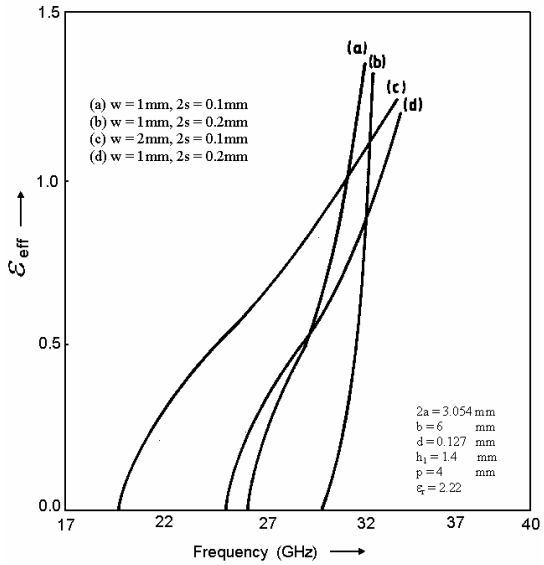

Figure 9. Dispersion of broadside-coupled stripline periodically loaded with series capacitive gaps.

that with wider strips, the width of first passband increase and that of first stopband decreases. Over the practical passband range, ε_{eff} has a value in the range of 0.0 to 1.5. Therefore this type of periodic configuration is no useful as a slow wave structure.

6. CONCLUSIONS

The suspended stripline with periodically loaded capacitive gaps is characterized by a lower cut-off frequency f_c for the first passband (Fig. 3). The structure offers very narrow passband and wide stopband, particularly when the strip pattern is in close proximity to either the bottom or topwall. In Figs. 5 and 6 the wider passband can be achieved by positioning strip conductor pattern at or close to the centre of the quide (curves b, c, d and e in Fig. 5 with $\varepsilon_r = 2.22$; the maximum value of ε_{eff} is less than about 1.5).

The characteristics of periodic broadside-coupled suspended stripline with the different periodic patterns are similar to the characteristic of the corresponding periodic structure in single conductor suspended stripline with symmetrically located substrate, in which the structure has a lower cut-off frequency, f_c, narrow passband, wide stopband and ε_r in an approximate range $0 \leq \varepsilon_{eff} \leq 1.5$ with patterns.

REFERENCES

1. Kiang, J. F., S. M. Ali, and J. A. Kong, "Propagation properties of striplines periodically with crossing strips," *IEEE Transactions on MTT*, Vol. 37, 776–786, April 1989.
2. Koal, S. K., "Millimeter wave circuit techniques and technology for radar and wireless communication," *Proc. 4th International Conference on Millimeter Wave and for Infrared Sience and Technology*, 206–209, Aug. 1996.
3. Packiaraj, D., M. Ramesh, and A. T. Kalghatgi, "Periodically loaded SSS coupled-line filter for second harmonic suppression," *Microwave Journal*, Vol. 49, No. 7, 106, July 2006.
4. Nenzel, W. and M. Sathiasealan, "Frequency scanned antenna array using a suspended stripline negative index transmission line," *Microwave Conference 2005 European*, Vol. 1, 4, Oct. 2005.
5. Fardis, M., B. Bhat, and S. K. Koul, "Double dielectric finline with slots periodically loaded with inductive strips," *Journal Electronics and Telecommunication Engineers*, Vol. 41, 31–38, Jan./Feb. 1995.

6. Tounsi, M. L., R. Touhami, and A. Khodja, "Analysis of the mixed coupling in bilateral microwave circuits anisotropy for MICs and MMICs applications," *Progress In Electromagnetics Research*, PIER 62, 281–315, 2006.
7. Jin, L., C. Ruan, and L. Chun, "Design E-plane bandpass filter based on EM-ANN mode," *Progress In Electromagnetics Research*, PIER 20, No. 8, 1061–1069, 2006.
8. Jin, L. and C.-L. Ruan, "Neural network models for finline discontinuties," *International Journal of Infrared and Millimeter Waves*, Vol. 25, No. 12, 1019–1027, 2004.
9. Casula, G. A., G. Mazzarella, and G. Montisci, "Effective analysis of a microstrip slot coupler," *Journal of Electromagnetic Waves and Applications*, Vol. 18, No. 9, 1203, 2004
10. Mirshekar-Syahkal, D. and J. B. Davies, "Accurate analysis of coupled strip-finline structure for phase constant, characteristic impedance, dielectric and conductor losses," *IEEE Trans. on Microwave Theory and Tech.*, Vol. 30, No. 6, 906–910, June 1982.
11. Itoh, T. and A. S. Hebert, "A generalized spectral domain analysis for coupled suspended microstriplines with tuning septums," *IEEE Trans. on Microwave Theory and Tech.*, Vol. 26, No. 10, 820–826, October 1978.